Global atmospheric oxygen variations recorded by Th/U systematics of igneous rocks

He Liu[a,b,c], Robert E. Zartman[a], Trevor R. Ireland[d], and Wei-dong Sun[a,b,c,1]

[a]Center of Deep-Sea Research, Institute of Oceanology, Chinese Academy of Sciences, 266071 Qingdao, China; [b]Laboratory for Marine Mineral Resources, Qingdao National Laboratory for Marine Science and Technology, 266237 Qingdao, China; [c]Center for Ocean Mega-Science, Chinese Academy of Sciences, 266071 Qingdao, China; and [d]Research School of Earth Sciences, Australian National University, Canberra, ACT 2601, Australia

Edited by Mark H. Thiemens, University of California at San Diego, La Jolla, CA, and approved August 5, 2019 (received for review February 16, 2019)

Atmospheric oxygen has evolved from negligible levels in the Archean to the current level of about 21% through 2 major step rises: The Great Oxidation Event (GOE) in the early Proterozoic and the Neoproterozoic Oxygenation Event (NOE) during the late Proterozoic. However, most previous methods for constraining the time of atmospheric oxygenation have relied on evidence from sedimentary rocks. Here, we investigate the temporal variations of the Th/U of arc igneous rocks since 3.0 billion y ago (Ga) and show that 2 major Th/U decreases are recorded at ca. 2.35 Ga and ca. 0.75 Ga, coincident with the beginning of the GOE and NOE. The decoupling of U from Th is predominantly caused by the significant rise of atmospheric oxygen. Under an increasingly oxidized atmosphere condition, more uranium in the surface environment became oxidized from the water-insoluble U^{4+} to the water-soluble U^{6+} valance and incorporated in the sea water and altered oceanic crust. Eventually, the subduction of this altered oceanic crust produced the low-Th/U signature of arc igneous rocks. Therefore, the sharp decrease of Th/U in global arc igneous rocks may provide strong evidence for the rise of atmospheric oxygen. We suggest that the secular Th/U evolution of arc igneous rocks could be an effective geochemical indicator recording the global-scale atmospheric oxygen variation.

Th/U systematics | arc igneous rocks | Great Oxidation Event | Neoproterozoic Oxygenation Event

Earth's atmosphere was initially almost devoid of oxygen with only minor evidence of the biological activity that would lead to the following build-up of oxygen (1–9). Geochemical indicators suggest that the rise of atmospheric oxygen proceeded in 2 major steps: the Great Oxidation Event (GOE) from ca. 2.4–2.1 billion years ago (Ga) (2, 4, 10–14) and the Neoproterozoic Oxygenation Event (NOE) around 0.8–0.63 Ga (7, 15–21).

Previous studies on the timing of the GOE and NOE depended largely on geochemical signatures from sedimentary rocks together with the first appearance or disappearance of redox-sensitive geological and paleontological indicators. Timing of the GOE is defined by the abrupt disappearance of non-mass-dependent (NMD) fractionation of sulfur isotopes in sedimentary rocks at 2.45–2.32 Ga (4, 10, 12, 22). The NOE is constrained by the considerable enrichments of Mo and V in shales since around 0.63 Ga (17, 18, 23) and a wide range of $\delta^{53}Cr$ values in some ca. 0.8–0.75 Ga shales (7), as well as some more controversial explanations of a negative carbon isotope excursion (24).

However, sedimentary rocks do not provide a complete and continuous record for the rise of atmospheric oxygen throughout Earth's history due to the lack of appropriate rock samples for some time intervals (3). Therefore, the timing of oxygenation determined from the sedimentary rock record will be subject to refinement through the discovery of new occurrences of sequences with appropriate age and preservation. On the other hand, igneous rocks may provide a more continuous record of geochemical evolution. Little previous effort has been made using the elemental analysis of igneous rocks for the timing of oxygenation, and the influence of atmospheric oxygenation on the chemistry of a deep magma is still controversial (25–29). In our work, we apply a statistical approach to assessing geochemical data of worldwide arc igneous rocks in order to establish the secular variation of Th/U through time. In so doing, the Th-U fractionation in these igneous rocks was found to be strongly related to the onset of the GOE and NOE. The relationship between statistical geochemical characteristics of arc igneous rocks and atmospheric oxygenation is interpreted in this paper. We propose that the Th/U of igneous rocks could be an effective indicator for the timing of Earth's oxygenation events—providing an opportunity for further study on variations of atmospheric oxygen over geological history.

Results

Th-U Fractionation. Th and U are highly incompatible elements that are partitioned into Earth's crust over geological history (30, 31). Th and U in their tetravalent states have very similar geochemical behaviors because of their similar ionic sizes and tetravalent states (32, 33). Compositional trends of Th and U concentrations (ppm) and Th/U vs. SiO_2 (wt%) of worldwide igneous rocks are shown in Fig. 1 (*SI Appendix*, Table S1). The mean values of Th and U concentrations present undulating variations relative to the SiO_2. The mean concentration of Th for each SiO_2 interval is invariably higher than U, but the patterns of Th and U concentrations appear to be parallel to each other. Both the Th and U concentrations initially decrease with SiO_2 contents from 40 to 50 wt%. This is attributed to the fact that low-silica mafic rocks are dominated by alkali basalts, which are enriched in incompatible elements due to low degrees of mantle melting. Then, above 50 wt% SiO_2, the effects of magma differentiation

Significance

Scientists have been working on the dating of atmospheric oxygenation in Earth's history for decades. However, most previous studies relied on evidence from sedimentary rocks. Here, we show that igneous rocks can also be linked with surface oxidation by a key geological process: plate subduction. We here make an attempt to apply the Th/U of worldwide arc igneous rocks as an indicator for the timing of atmospheric oxygenation over the Earth's history. The results are coincident with the previously defined Great Oxidation Event and Neoproterozoic Oxygenation Event.

Author contributions: W.-d.S. designed research; H.L. and W.-d.S. performed research; H.L. analyzed data; and R.E.Z., T.R.I., and W.-d.S. wrote the paper.

The authors declare no conflict of interest.

This article is a PNAS Direct Submission.

This open access article is distributed under Creative Commons Attribution-NonCommercial-NoDerivatives License 4.0 (CC BY-NC-ND).

Data deposition: The compiled dataset and MATLAB code are freely available on GitHub at https://github.com/Codrlocas/Oxygen.git.

[1]To whom correspondence may be addressed. Email: weidongsun@qdio.ac.cn.

This article contains supporting information online at www.pnas.org/lookup/suppl/doi:10.1073/pnas.1902833116/-/DCSupplemental.

Published online September 3, 2019.

Downloaded at Australian Natl Univ on November 5, 2019

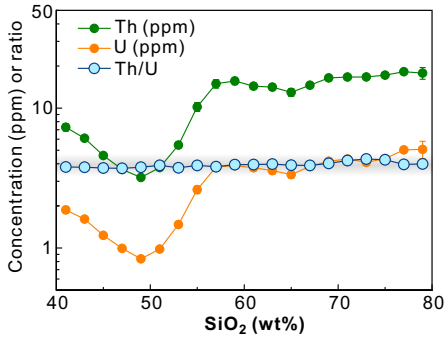

Fig. 1. Compositional trends of Th–SiO_2, U–SiO_2, and Th/U–SiO_2 for over 29,000 igneous rocks. The mean values of Th, U, and Th/U with SiO_2 concentrations ranging from 40 to 80 wt% were created by using IBM SPSS Statistics (Version 24). The bin size is set at 2 wt% SiO_2. Error bars show 2 SEs. Th and U concentrations show parallel variations in concentration from 40 to 80 wt% SiO_2, while the Th/U values are relatively constant within a small range throughout.

cause the Th and U concentrations to increase. Moreover, the average Th/U values with different silica contents are relatively constant (Fig. 1). Therefore, we conclude that Th and U are not significantly fractionated relative to each other with silica contents of the rocks.

In contrast, Th and U show very different behaviors where involved in supergene processes under an oxygen-rich atmosphere. The recycling of U from crust to mantle after the GOE has been discussed by previous studies and considered as the major cause of the second Pb paradox (32–35). Uranium is a redox-sensitive element with 2 major valence states, the water-soluble U^{6+} and water-insoluble U^{4+} (36), as well as the less-common U^{5+} state (37). On the other hand, Th has only 1 valence state, Th^{4+} (33, 38). In igneous rocks, U typically occurs in the water-insoluble U^{4+} valence state, the same as Th, and their behaviors are closely associated. Under an oxic atmospheric condition, weathering oxidizes the U^{4+} into U^{6+} (23, 38). The water-soluble U^{6+} then stays in solution in surface fluvial water, commonly in the stable and highly soluble form of uranyl carbonate complex $[UO_2(CO_3)_3^{4-}$ (39]), and is ultimately transported to the offshore and ocean environment (34). In contrast, Th^{4+} can only be transported with the river water and into the oceans as suspended particles from the physical weathering of surface rocks due to its insolubility in water (38). This accounts for the extremely low average Th/U of river water (commonly <0.1) and seawater (commonly $<10^{-3}$) (40) in contrast to that of the upper continental crust (Th/U = ~3.89) (31).

After transport of U into the open ocean, the most significant consequence is that the upper oceanic crust may become highly enriched in U due to seafloor alteration. Staudigel et al. (41) reported on the trace element compositions of altered basaltic upper oceanic crust from the Deep Sea Drilling Project sites 417 and 418 in the west Atlantic Ocean, indicating that the average Th/U in the altered upper oceanic crust can be as low as 0.33, much lower than the average Th/U of ~2.5–2.7 for unaltered midocean ridge basalt (MORB) (30, 42, 43). It has been suggested that the low Th/U signature of altered oceanic crust can be transferred into the deep mantle as well as the mantle wedge (33, 44). Although the amounts of Th and U migrating into the mantle wedge may only account for a small proportion to the total of subducted Th and U materials, they still can lower the average Th/U in the arc igneous rocks, especially for the oceanic arcs with relatively little contribution from the continental crust, in comparison to other tectonic settings.

We extracted the igneous data for the East Asia and northern Pacific with ages younger than 10 Ma from the EarthChem rock database (45) and plotted them on a map (Fig. 2*A*) to reveal the difference in Th/U between the arc and continental igneous rocks. The reason to choose such young rocks is that their current locations most closely represents the geological settings where they formed. The igneous rocks along the Alaska Peninsula, Aleutian Islands, Kamchatka Peninsula, Kuril Islands, and Izu–Bonin–Mariana Arc contain lower Th/U than the rocks from the Asian continent (Fig. 2*A*). We suggested that the oceanic arc rocks inherit the low Th/U signature of altered upper oceanic crust, while the relatively high-Th/U continental igneous rocks are less influenced by the subduction of oceanic slab. Instead, they perhaps are strongly affected or dominated by partial melting of the sublithospheric mantle or the middle-lower continental crust, of which the Th/U are much higher than that of the altered oceanic crust. Some arc rocks near the continent (e.g., Japanese archipelago, Ryukyu Islands, etc.) contain relatively higher Th/U than those from oceanic arcs, so that the range of Th/U of arc rocks (mostly 1–5) is partly overlapped with that of intracontinental rocks (mostly 3–10) (Fig. 2*B*). We attribute it to the contribution of melting of subducted sediments. It is noteworthy that the U concentrations of both arc and continental igneous rocks lie in a similar range (Fig. 2*B*), implying that the subduction of altered oceanic crust could only lower the Th/U rather than elevate the U concentrations in rocks, which are largely dependent on their silica contents (Fig. 1) and other igneous processes, such as the fractional crystallization of zircon, apatite, monazite, etc.

Another consequence of the increase of U concentration in the ocean is that the U^{6+} can be reduced back into immobile U^{4+}, probably in the form of fine-grained uraninite (UO_2), under locally anoxic conditions in the deep ocean and sequestered into organic-rich shale (23, 46). Although the U-enriched shales only account for a limited portion of the seafloor, they contain a substantial fraction of the overall U sink in the modern ocean (~27–40% of the riverine flux) (47). However, the shales are commonly deposited on the continental shelves, which are not normally subducted. We infer that the decrease of average Th/U in global-scale arc igneous rocks is predominantly caused by the subduction of altered oceanic crust.

Secular Th/U Variation through Time. We compiled a dataset including >29,000 igneous rocks spanning the last 3.0 Ga, extracted from the EarthChem database (45) with appropriate filtering (*Materials and Methods*). In order to check the Th/U variations of global-scale arc igneous rocks through time, we screened the data using several geochemical criteria of typical arc rocks, such as the intermediate-felsic lithologies, low Nb/Th, and low Th concentrations (*SI Appendix*, Figs. S1–S3; see *Materials and Methods* for details). All Th/U ratios throughout this report are given in their present-day values without correction for radioactive decay subsequent to the rock's formation. The average Th/U for arc rocks from 3.0 to 0 Ga was calculated by using the bootstrap method based on MATLAB encoding, creating the secular Th/U trend of arc igneous rocks through time (Fig. 3*A* and *SI Appendix*, Table S2). This curve is compared to the atmospheric oxygenation events in Earth's history in Fig. 3*E*. Prior to 2.35 Ga, the average Th/U gradually increased from ~3.8 to ~4.6. For the period from 2.35 to 2.05 Ga, the average Th/U dropped dramatically to ~2.1 and then returned to a level approximately equal to the Th/U value at 2.35 Ga. During the middle time of the Proterozoic between 2.05 and 0.75 Ga, the trajectory of Th/U varied in an oscillating style and reached a value of ~4.7 at ca. 0.75 Ga. At 0.75–0.65 Ga, Th/U decreased significantly, with the lowest value of ~3.3 occurring at 0.65 Ga. After 0.65 Ga, Th/U gradually increased again over time and reached a value of ~4.0 for the last 0.1 Ga.

Downloaded at Australian Natl Univ on November 5, 2019

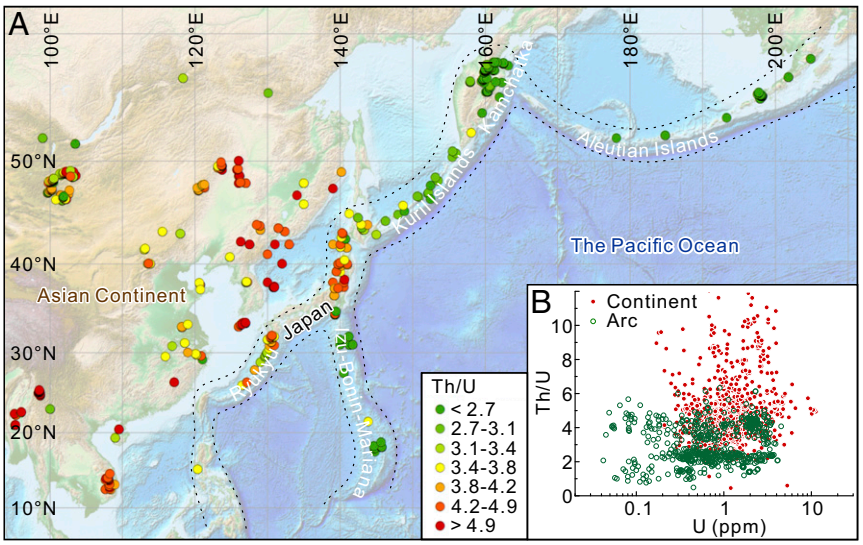

Fig. 2. The Th/U of igneous rocks (younger than 10 Ma) in the East Asian continent and northern Pacific. (*A*) A map showing the Th/U of igneous rocks. The green–yellow–red filled circles represent the levels of Th/U. Black dashed lines subdivided the igneous rocks into continental and arc groups, respectively. Adapted with permission from ref. 73. (*B*) Scatter plots of Th/U vs. U concentrations for continental and arc rocks, respectively. The Th/U values of arc rocks (green hollow circles) are generally lower than those of intracontinental rocks (red points).

Discussion

The GOE. Before the GOE, the atmosphere was very anoxic [<0.001% of the present atmospheric level (PAL)] (7, 11), which is demonstrated by the large NMD fractionation of sulfur isotopes that is prevalent in the Archean (Fig. 3*D*) (10–12, 22, 48), as well as the broad existence of detrital uraninites (23), pyrites (11, 49), and banded iron formations (50, 51). Under such an anoxic atmosphere, U existed mostly in the U^{4+} valance state in near-surface environments, especially in the form of uraninite (UO_2). For instance, detrital uraninite grains were found in Witwatersrand quartz-pebble conglomerates (3.0–2.7 Ga) in South Africa (52) and in the Mesoarchean (3.2–2.8 Ga) sediments from the Australian Pilbara Craton (38). Uranium was not decoupled from Th before the GOE by supergene process because the recycling mechanisms of both Th^{4+} and U^{4+} operating from the surface down to the depth of arc igneous rocks were identical. The altered oceanic crust during that time probably did not have a low Th/U, either. However, we observed a gradual increasing trend of the average Th/U in arc igneous rocks from 3.0 to 2.35 Ga (Fig. 3*A*). Since there is no evidence that the atmosphere–ocean system became more reducing over time before the GOE, we surmise that the increasing Th/U of arc igneous rocks is probably attributed to the gradually decreasing degree of mantle melting (53) as a consequence of the progressive cooling of the mantle. Such a cooling trend of the mantle from the early Archean to the present is now widely accepted (54–56). A related temporal trend to the degrees of melting of the mantle has also been proposed (57) (Fig. 3*A* and *SI Appendix*, Fig. S4*B*). The plotting of the Rittmann Index (σ), a petrological indicator associated with the degrees of mantle melting (58), of arc rocks through time also shows a decreasing trend of melting degrees since ca. 3.0 Ga (*SI Appendix*, Fig. S4*A*). To verify the correlation between the Th/U in arc rocks and melting degree, we calculated the average Th/U for rocks with different Rittmann Index (σ). The results show that the Th/U in global-scale arc igneous rocks positively correlates with the Rittmann Index (σ) (Fig. 4 and *SI Appendix*, Table S3). Therefore, the increasing trend of Th/U in arc rocks from 3.0 to 2.35 Ga (Fig. 3*A*) is consistent with the gradually decreasing degree of mantle melting (57). Based on this observation, we modeled a presumed trajectory of average Th/U in arc rocks through time in accordance with the previously proposed trend of the apparent melting degrees of the mantle (57). This presumed Th/U curve is independent of the Th–U fractionation caused by surface oxidation.

The abnormally low Th/U signatures during the GOE (Fig. 3*A*) indicate that the U was abruptly elevated in arc igneous rocks relative to Th. After the onset of the GOE around 2.43 Ga (59), the surficial U^{4+}, especially in detrital uraninite grains in fluvial sediments, was rapidly oxidized into U^{6+}, owing to the increasingly oxidized atmospheric condition. It could then be dissolved into the rivers and transported to the oceans. Weathering under the oxygen-rich atmosphere was also enhanced. The general disappearance of detrital uraninite record in the sedimentary rocks younger than 2.2 Ga (38) suggests that atmospheric oxygen had been elevated to over ∼1% of the PAL (23), so that the surface-exposed detrital uraninite grains were no longer stable (38). The rapid dissolution of uraninites might have led to an accumulation of considerable U^{6+} in the seawater at the beginning of the GOE and resulted in the abrupt decrease of Th/U in the upper oceanic crust through seafloor alteration. This is consistent with the sharp increase of U concentrations in shales during the GOE (23) (Fig. 3*B*). Consequently, the arc igneous rocks revealed a remarkably low Th/U signature commencing at ca. 2.35 Ga (Fig. 3*A*) due to subduction of the U-altered oceanic crusts, although there would be a delay between the surface oxidation and the subduction of the near-trench altered oceanic crust with low-Th/U signature.

Arc rocks formed during the GOE have been reported from the Niani area of northeast Guinea (60), the Sao Luis Craton of northern Brazil (61), and the North China Craton (62, 63). The trace-element spider diagrams of these rocks (*SI Appendix*, Fig. S5) show relative enrichment of fluid-mobile elements (e.g., Rb, La, U, etc.) and depletion of high-field-strength elements (such as Nb, Ta, and Ti), typical of island-arc or active continental margin settings (60, 61). The average Th/U of these rocks is as low as about 2.6, which contributes to the Th/U excursion in the 2.35- to 2.05-Ga interval shown in Fig. 3*A*.

The Th/U of arc igneous rocks rapidly returned to the level of the presumed oxidation-independent Th/U trend at ca. 2.05 Ga (Fig. 3*A*), so that the low Th/U became a distinguishable transient excursion of the GOE. Given a constant riverine U flux to the oceans after the GOE (23), the most plausible reason for this

Downloaded at Australian Natl Univ on November 5, 2019

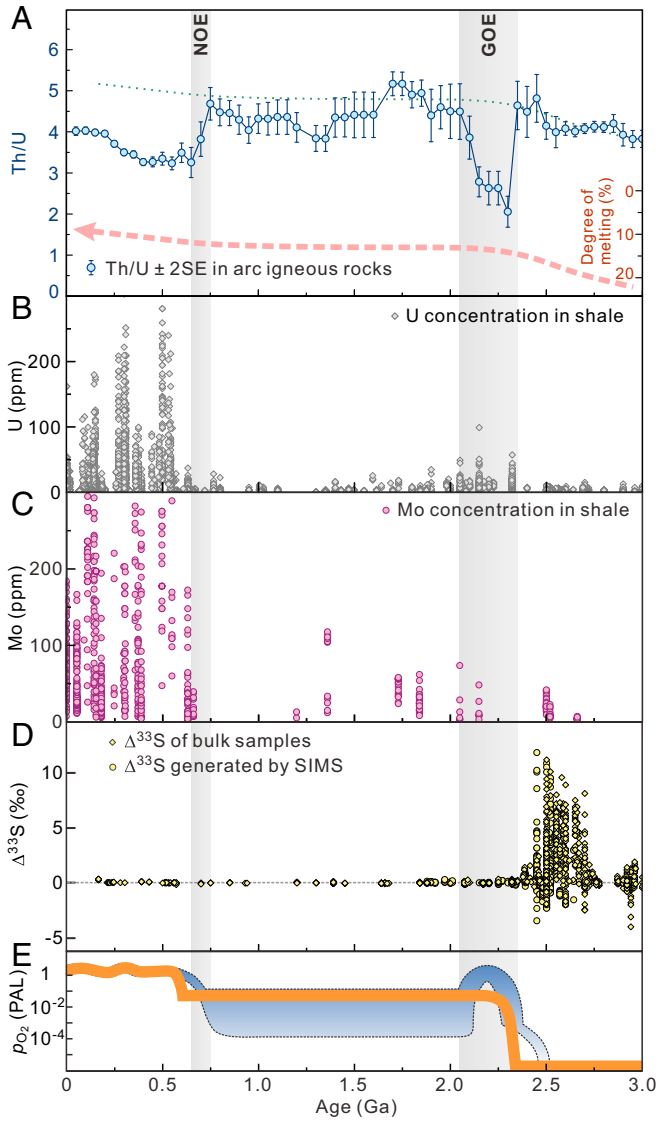

Fig. 3. Secular variations of redox-sensitive geochemical indicators throughout Earth's history. (*A*) Secular Th/U evolution of worldwide arc igneous rocks from 3.0 to 0 Ga. Error bars denote 2 SEs. The major Th/U decreases occur at 2.35 and 0.75 Ga, coincident with the onset times of the GOE and NOE. The pink dashed curve shows the simplified trend of the degrees of mantle melting estimated by Keller and Schoene (57) (*SI Appendix*, Fig. S4*B*). The green dotted curve parallel to the pink dashed curve is a presumed oxidation-independent Th/U trend through time. (*B*) U concentrations in organic-rich shales over time (23). (*C*) Mo concentrations in shales (17, 18). (*D*) NMD fractionation of S isotopes in sedimentary rocks (74). The permanent disappearance of NMD signatures is symptomatic of the rise of atmospheric oxygen during the GOE. (*E*) Evolution of Earth's atmospheric oxygen content through time. The orange and blue bands are suggested by refs. 3 and 4. pO_2 (PAL), atmospheric partial pressure of oxygen relative to the PAL.

phenomenon may be the previously recognized remarkable deoxygenation occurring at the end of the 2.22- to 2.06-Ga Lomagundi Event (4, 5, 14, 64). The fall in the oxygen level of the atmosphere–ocean system after the GOE and Lomagundi Event led to expanded anoxia in ocean settings (5, 14, 64). Consequently, dissolved U was distributed or removed into a large U sink, resulting in low U concentration in the seawater and even in the deep-ocean water (23). This is consistent with the fall of U concentrations in shales after the GOE (23). A noteworthy phenomenon is that the average Th/U in arc igneous rocks during the GOE was even lower than that in younger Phanerozoic arc rocks. We attribute this curiosity to the relatively higher degrees of mantle melting in the Paleoproterozoic than those in the Phanerozoic (54, 55).

The atmospheric oxygen level during the period between the GOE and NOE is estimated at from <0.1% to >4% of present level (4, 7, 65–67). Under such low-oxygen atmospheric environments, the U concentrations in the seawater were still at very low levels, as illustrated by the U concentrations in similar aged shales (23). This accounts for the average Th/U in the 2.05- to 0.75-Ga arc igneous rocks being approximately equal to the presumed oxidation-independent Th/U trend (Fig. 3*A*). This fact also implies a widespread anoxic atmosphere–ocean system between the GOE and NOE, even though the atmospheric oxygen level during that time was higher than it was in the pre-GOE time (<0.001% of PAL). There was some minor fluctuation of Th/U during this period, but negligible within 2 SEs.

The NOE. A stepwise Th/U decrease of global arc igneous rocks occurred in the 0.75- to 0.65-Ga interval (Fig. 3*A*), which corresponds to the second major rise in atmospheric oxygen over the Earth's history, the NOE. The beginning time of the NOE has been defined as ~0.8–0.63 Ga by the enormous increases of V and Mo concentrations in Ediacaran and Phanerozoic shales (18, 23) (Fig. 3 *B* and *C*), as well as a wide range of $\delta^{53}Cr$ values in the ca. 0.8- to 0.75-Ga shales (7), which approximately coincided with the Th/U decrease of arc rocks at 0.75–0.65 Ga (Fig. 3*A*). The recurring sharp decrease of the Th/U of global arc igneous rocks at this time suggests a further U enhancement in the altered oceanic crust, as well as a substantial growth in the oceanic U reservoir. This was a consequence of the dramatically increased oxygen content in the atmosphere–ocean system during the NOE.

Subsequent to the termination of the NOE, the atmospheric oxygen amount had been elevated to much higher levels, which led up to the rise of animal life (4, 15, 68). The oxidized ocean dissolved more water-soluble U^{6+} in the seawater and deep-ocean water and incorporated it into the altered oceanic crust. This low-Th/U altered oceanic curst could then be recycled into the arc igneous rocks during the process of plate subduction. This would then contribute to the overall lower Th/U observed in the Phanerozoic arc rocks than the modeled oxidation-independent Th/U trend (Fig. 3*A*). The average Th/U in arc rocks gradually increased through time after the NOE, which could also be ascribed to the decreasing degree of mantle melting (*SI Appendix*, Fig. S4) (57). Although it seems that the Th/U in arc rocks increased a little faster than the modeled Th/U trend, the current evidence is not sufficient to make a confident interpretation because the evolution of the degrees of mantle melting during the Phanerozoic is only roughly constrained.

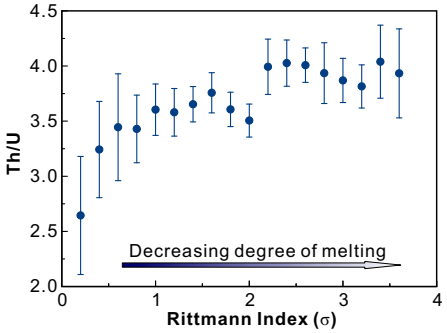

Fig. 4. Error bar plots of Th/U vs. Rittmann Index (σ) in arc igneous rocks. $\sigma = (Na_2O + K_2O)^2/(SiO_2\text{-}43)$, units in wt% (58). Error bars denote 2 SEs. The bin size is 0.2.

Downloaded at Australian Natl Univ on November 5, 2019

An Effective Indicator for the Timing of Atmospheric Oxygenation. Scientists have been working on the timing of atmospheric oxygenation in the Earth's history for several decades. However, most previous studies have relied on evidence from sedimentary rocks. Almost no previous attempt has been made to constrain the times of atmospheric oxygenation events using the element composition of igneous rocks. A recent study using the Th/U in MORB to monitor crust–mantle differentiation provides evidence of limited crustal recycling following the GOE (29). In our study, we have determined that the decreases in Th/U of worldwide arc igneous rocks are substantially associated with known atmospheric oxygenation events. Under an increasingly oxidized atmosphere condition, U has been decoupled from Th during oxidation and weathering processes at the Earth's surface and is preferentially incorporated into altered upper oceanic crust (33, 34, 38). Then, the low Th/U signature within the altered oceanic crust is recycled into the mantle wedge through plate subduction, causing a decrease in Th/U of arc igneous rocks.

The accurate ages of Precambrian sedimentary rocks are often difficult to determine, unless there are shales for which rhenium–osmium (Re-Os) isochron dating can be applied, or there is a contemporaneous dateable volcanic unit available. In comparison, igneous rocks have been more thoroughly analyzed, and there are more samples available. In terms of an intermediate-felsic arc igneous rock, there is the potential for dating the rocks far more accurately. Although there is a potential lag time, as the altered oceanic crust requires recycling into the igneous sources, the beginning times of the GOE and NOE estimated by the decreases in Th/U in arc rocks, ∼2.35 and 0.75 Ga, are no more than 50–100 Ma later than the so far defined earliest times of those 2 events, ∼2.43 Ga (59) and ∼0.8 Ga (7, 19, 20), respectively.

The starting time of the GOE was originally defined by the abrupt disappearance of NMD sulfur isotope fractionations in sedimentary rocks (10). Since the atmospheric oxygen level increased during the GOE, there has been no NMD fingerprint since. The starting time of the later NOE cannot be determined by NMD sulfur fractionation, and, thus, as a substitution has been defined by the strong enrichments of V and Mo in shales. Here, we propose that the worldwide trend of secular Th/U variations in arc igneous rocks may now be used as a single geochemical indicator to reflect the entire history of atmospheric oxygenation, including a separation of the effects of the GOE from those of the NOE. The interpretation of this Th/U record may be still quite speculative, but the observation appears to be quite robust.

Conclusions

The Th/U is a key indicator in understanding the long-term oxygen evolution of planet Earth. The decoupling of U from Th in arc igneous rocks is predominantly attributed to the significant rise of atmospheric oxygen. Under an increasingly oxidized atmosphere, U is fractionated from Th by surface oxidation and preferentially incorporated into the altered oceanic crust, which are eventually subducted and recycled into the mantle wedge. Therefore, the atmospheric oxygenation event occurring throughout Earth's history can be recognized by the dramatically lowered average Th/U in arc igneous rocks.

The Th/U in arc rocks can provide a temporal record for the rise of atmospheric oxygen. In this study, 2 remarkable Th/U decreases occurring at 2.35 and 0.75 Ga were determined to be generally coincident with the onsets of the GOE and NOE, indicating the effectiveness of the Th/U in arc rocks for the timing of atmospheric oxygenation events.

Materials and Methods

Data Preparation. Geochemical data of igneous rocks were downloaded from the freely accessible EarthChem rock database (45). The data structure includes ages, longitude–latitude coordinates, lithology, and data sources. Rock samples with age uncertainty larger than 100 Ma were not included in the data used for assessment. In order to obtain a balanced record of the tectonic settings of the rocks through time, we removed all those samples derived from the oceanic floor (including midocean ridges, oceanic islands, oceanic basins, seamounts, etc.) (*SI Appendix*, Fig. S6) because these rocks are all typically younger than 200 Ma, while preservation of old oceanic igneous rocks is much less common due to plate subduction. Samples with ages greater than 3.0 Ga were also removed because the record for this epoch is rather incomplete and subject to additional statistical uncertainty. Besides, igneous rocks older than 3.0 Ga might form under a different tectonic regime, as suggested by many researchers (69–71). To obtain accurate statistical results, we removed all of the analytical values of Th and U assayed by X-ray fluorescence methods. For this evaluation, we extracted a total of 29,496 igneous rocks, along with their major and trace element concentrations (72). The data density in each 50-Ma time interval from 3.0 Ga to the present was also taken into account (*SI Appendix*, Fig. S7). The number of Precambrian rock samples is much less than that of the Phanerozoic. Some of the Precambrian time intervals lack igneous rocks with Th and U data, and particularly for periods such as 2.4–2.25 Ga, 1.5–1.4 Ga, etc. The mean Th/U for those unrepresented time intervals was interpolated by using the rocks of adjacent ages through the central moving average method.

Screening for Arc Igneous Rocks. We used several criteria to screen the arc igneous rocks in the dataset through the following steps. *1*) We checked all of the silica contents of igneous rocks younger than 10 Ma sampled from the East Asia and the western border of the Pacific Ocean (*SI Appendix*, Fig. S1). The frequency histograms of SiO_2 contents (wt%) of those rocks indicated that the arc rocks contain variable SiO_2 contents from 46 to 77 wt%, while the intracontinental rocks predominantly contain <54 wt% SiO_2. Thus, we filtered out the rocks with SiO_2 contents less than 54 wt% to avoid intracontinental basaltic rocks and only kept intermediate-felsic rocks (≥54 wt% SiO_2) for the next step. *2*) Since the subduction-related igneous rocks are commonly characterized by negative Nb anomaly, we created the frequency histograms of Nb/Th for the intermediate-felsic rocks from arc, intracontinent, collisional orogen (the Tibetan Plateau), and continental rift (the East African Rift), respectively (*SI Appendix*, Fig. S2). The results revealed that the intracontinental and continental rift rocks can be mostly filtered out by $\log_{10}$ Nb/Th > 0.7 (or Nb/Th > 5). However, the Nb/Th histograms of arc and collisional orogenic rocks were considerably overlapped. We selected the rocks with $\log_{10}$ Nb/Th ≤ 0.7 and proceeded to the next step. *3*) We compared the frequency histograms of Th concentrations in rocks from the arc and collisional orogen and noticed that the collisional orogenic rocks can be largely distinguished from arc rocks by the criterion of $\log_{10}$ Th > 1.1 ppm (or Th > 12.6 ppm) (*SI Appendix*, Fig. S3). Through the above 3 steps of data screening by MATLAB encoding, the remaining dataset comprises predominantly arc rocks and is ready for the calculation of secular Th/U variation in arc rocks through time.

Statistical Analysis. We created the error bar plots for Th and U concentrations (ppm) as well as the Th/U against SiO_2 concentrations (wt%) for the whole dataset using IBM SPSS Statistics (Version 24) to derive the Th–SiO_2, U–SiO_2, and Th/U–SiO_2 compositional trends (Fig. 1 and *SI Appendix*, Table S1).

The average Th/U values from 3.0 to 0 Ga were calculated by using the bootstrap method based on MATLAB (Version R2014a) encoding. A central moving average smoothing was applied to determine mean values due to the lack of sufficient data for certain time intervals. The width of the sample window was set at 0.2 Ga, while the step width was set at 0.05 Ga. Thus, the results for the timing have an uncertainty of ±0.1 Ga. To remove the abnormal extreme values, only the middle 95% of data was calculated for the means and SEs. We executed 10,000 iterations for bootstrap resampling. Rocks younger than 0.1 Ga were not employed in the calculation, as those rocks included a large proportion of samples from oceanic arcs, which were relatively less preserved than the continental arc samples before 0.1 Ga, especially in Precambrian time. The results are shown in Fig. 3*A* and *SI Appendix*, Table S2.

The data and computer code supporting the findings of this study are available in *SI Appendix* (Datasets S1 and S2).

ACKNOWLEDGMENTS. This study was supported by Strategic Priority Research Program of the Chinese Academy of Sciences (CAS) Grant XDB18020102 and National Key R & D Program of China Grant 2016YFC0600408 (to W.-d.S.). T.R.I. acknowledges a CAS President visiting fellowship. We thank Prof. Charles Langmuir for his suggestions and Al Hofmann and Andrey Bekker for constructive review comments.

Downloaded at Australian Natl Univ on November 5, 2019

1. I. H. Campbell, C. M. Allen, Formation of supercontinents linked to increases in atmospheric oxygen. *Nat. Geosci.* **1**, 554–558 (2008).
2. H. D. Holland, Why the atmosphere became oxygenated: A proposal. *Geochim. Cosmochim. Acta* **73**, 5241–5255 (2009).
3. L. R. Kump, The rise of atmospheric oxygen. *Nature* **451**, 277–278 (2008).
4. T. W. Lyons, C. T. Reinhard, N. J. Planavsky, The rise of oxygen in Earth's early ocean and atmosphere. *Nature* **506**, 307–315 (2014).
5. F. Ossa Ossa *et al*., Two-step deoxygenation at the end of the Paleoproterozoic Lomagundi Event. *Earth Planet. Sci. Lett.* **486**, 70–83 (2018).
6. F. Ossa Ossa *et al*., Limited oxygen production in the Mesoarchean ocean. *Proc. Natl. Acad. Sci. U.S.A.* **116**, 6647–6652 (2019).
7. N. J. Planavsky *et al*., Earth history. Low mid-Proterozoic atmospheric oxygen levels and the delayed rise of animals. *Science* **346**, 635–638 (2014).
8. R. S. Hiebert, A. Bekker, M. G. Houlé, O. J. Rouxel, Depositional setting of the Late Archean Fe oxide- and sulfide-bearing chert and graphitic argillite in the Shaw Dome, Abitibi Greenstone Belt, Canada. *Precambrian Res.* **311**, 98–116 (2018).
9. B. Eickmann *et al*., Isotopic evidence for oxygenated Mesoarchaean shallow oceans. *Nat. Geosci.* **11**, 133–138 (2018).
10. A. Bekker *et al*., Dating the rise of atmospheric oxygen. *Nature* **427**, 117–120 (2004).
11. H. D. Holland, The oxygenation of the atmosphere and oceans. *Philos. Trans. R. Soc. Lond. B Biol. Sci.* **361**, 903–915 (2006).
12. J. Farquhar, J. Savarino, T. L. Jackson, M. H. Thiemens, Evidence of atmospheric sulphur in the martian regolith from sulphur isotopes in meteorites. *Nature* **404**, 50–52 (2000).
13. J. A. Karhu, H. D. Holland, Carbon isotopes and the rise of atmospheric oxygen. *Geology* **24**, 867–870 (1996).
14. N. J. Planavsky, A. Bekker, A. Hofmann, J. D. Owens, T. W. Lyons, Sulfur record of rising and falling marine oxygen and sulfate levels during the Lomagundi event. *Proc. Natl. Acad. Sci. U.S.A.* **109**, 18300–18305 (2012).
15. D. E. Canfield, S. W. Poulton, G. M. Narbonne, Late-Neoproterozoic deep-ocean oxygenation and the rise of animal life. *Science* **315**, 92–95 (2007).
16. D. A. Fike, J. P. Grotzinger, L. M. Pratt, R. E. Summons, Oxidation of the Ediacaran ocean. *Nature* **444**, 744–747 (2006).
17. C. Scott *et al*., Tracing the stepwise oxygenation of the Proterozoic ocean. *Nature* **452**, 456–459 (2008).
18. S. K. Sahoo *et al*., Ocean oxygenation in the wake of the Marinoan glaciation. *Nature* **489**, 546–549 (2012).
19. D. Thomson, R. H. Rainbird, N. Planavsky, T. W. Lyons, A. Bekker, Chemostratigraphy of the Shaler Supergroup, Victoria Island, NW Canada: A record of ocean composition prior to the Cryogenian glaciations. *Precambrian Res.* **263**, 232–245 (2015).
20. E. C. Turner, A. Bekker, Thick sulfate evaporite accumulations marking a mid-Neoproterozoic oxygenation event (Ten Stone Formation, Northwest Territories, Canada). *Geol. Soc. Am. Bull.* **128**, 203–222 (2015).
21. C. T. Reinhard *et al*., Evolution of the global phosphorus cycle. *Nature* **541**, 386–389 (2017).
22. J. Farquhar *et al*., Isotopic evidence for Mesoarchaean anoxia and changing atmospheric sulphur chemistry. *Nature* **449**, 706–709 (2007).
23. C. A. Partin *et al*., Large-scale fluctuations in Precambrian atmospheric and oceanic oxygen levels from the record of U in shales. *Earth Planet. Sci. Lett.* **369**, 284–293 (2013).
24. N. L. Swanson-Hysell *et al*., Cryogenian glaciation and the onset of carbon-isotope decoupling. *Science* **328**, 608–611 (2010).
25. C. T. Lee *et al*., The redox state of arc mantle using Zn/Fe systematics. *Nature* **468**, 681–685 (2010).
26. Z.-X. Anser Li, C.-T. Aeolus Lee, The constancy of upper mantle fO2 through time inferred from V/Sc ratios in basalts. *Earth Planet. Sci. Lett.* **228**, 483–493 (2004).
27. M. Brounce, E. Stolper, J. Eiler, Redox variations in Mauna Kea lavas, the oxygen fugacity of the Hawaiian plume, and the role of volcanic gases in Earth's oxygenation. *Proc. Natl. Acad. Sci. U.S.A.* **114**, 8997–9002 (2017).
28. K. A. Kelley, E. Cottrell, Water and the oxidation state of subduction zone magmas. *Science* **325**, 605–607 (2009).
29. S. A. Wipperfurth, M. Guo, O. Šrámek, W. F. McDonough, Earth's chondritic Th/U: Negligible fractionation during accretion, core formation, and crust–mantle differentiation. *Earth Planet. Sci. Lett.* **498**, 196–202 (2018).
30. A. W. Hofmann, Chemical differentiation of the Earth: The relationship between mantle, continental crust, and oceanic crust. *Earth Planet. Sci. Lett.* **90**, 297–314 (1988).
31. R. L. Rudnick, S. Gao, "4.1–Composition of the continental crust" in *Treatise on Geochemistry*, H. D. Holland, K. K. Turekian, Eds. (Elsevier, Oxford, ed. 2, 2014), pp. 1–51.
32. R. E. Zartman, S. M. Haines, The plumbotectonic model for Pb isotopic systematics among major terrestrial reservoirs—A case for bi-directional transport. *Geochim. Cosmochim. Acta* **52**, 1327–1339 (1988).
33. T. Elliott, A. Zindler, B. Bourdon, Exploring the kappa conundrum: The role of recycling in the lead isotope evolution of the mantle. *Earth Planet. Sci. Lett.* **169**, 129–145 (1999).
34. K. D. Collerson, B. S. Kamber, Evolution of the continents and the atmosphere inferred from Th-U-Nb systematics of the depleted mantle. *Science* **283**, 1519–1522 (1999).
35. R. E. Zartman, S. H. Richardson, Evidence from kimberlitic zircon for a decreasing mantle Th/U since the Archean. *Chem. Geol.* **220**, 263–283 (2005).
36. C. E. Barnes, J. K. Cochran, Uranium removal in oceanic sediments and the oceanic-U balance. *Earth Planet. Sci. Lett.* **97**, 94–101 (1990).
37. P. C. Burns, R. J. Finch, Wyartite: Crystallographic evidence for the first pentavalent-uranium mineral. *Am. Mineral.* **84**, 1456–1460 (1999).
38. R. M. Hazen, R. C. Ewing, D. A. Sverjensky, Evolution of uranium and thorium minerals. *Am. Mineral.* **94**, 1293–1311 (2009).
39. D. Langmuir, Uranium solution-mineral equilibria at low temperatures with applications to sedimentary ore deposits. *Geochim. Cosmochim. Acta* **42**, 547–569 (1978).
40. P. S. Andersson, G. J. Wasserburg, J. H. Chen, D. A. Papanastassiou, J. Ingri, 238U234U and232Th230Th in the Baltic Sea and in river water. *Earth Planet. Sci. Lett.* **130**, 217–234 (1995).
41. H. Staudigel, T. Plank, B. White, H. U. Schmincke, "Geochemical fluxes during seafloor alteration of the basaltic upper oceanic crust: DSDP Sites 417 and 418" in *Subduction Top to Bottom*, G. E. Bebout, D. W. Scholl, S. H. Kirby, J. P. Platt, Eds. (Geophysical Monograph Series, American Geophysical Union, Washington, DC, 1996), **vol. 96**, pp. 19–38.
42. S. S. Sun, W. F. McDonough, "Chemical and isotopic systematics of oceanic basalts: Implications for mantle composition and processes" in *Magmatism in the Ocean Basins*, A. D. Saunders, M. J. Norry, Eds. (Geological Society Special Publications, Geological Society of London, London, U.K., 1989), **vol. 42**, pp. 313–345.
43. W. M. White, E. M. Klein, "4.13–Composition of the oceanic crust" in *Treatise on Geochemistry*, H. D. Holland, K. K. Turekian, Eds. (Elsevier, Oxford, U.K., ed. 2, 2014), pp. 457–496.
44. M. B. Andersen *et al*., The terrestrial uranium isotope cycle. *Nature* **517**, 356–359 (2015).
45. EarthChem, Portal Search. www.earthchem.org/portal. Accessed 9 August 2018 (Interdisciplinary Earth Data Alliance, Palisade, NY, 2017).
46. C. E. Barnes, J. K. Cochran, Uranium geochemistry in estuarine sediments–Controls on removal and release processes. *Geochim. Cosmochim. Acta* **57**, 555–569 (1993).
47. R. M. Dunk, R. A. Mills, W. J. Jenkins, A reevaluation of the oceanic uranium budget for the Holocene. *Chem. Geol.* **190**, 45–67 (2002).
48. D. E. Canfield, K. S. Habicht, B. Thamdrup, The Archean sulfur cycle and the early history of atmospheric oxygen. *Science* **288**, 658–661 (2000).
49. D. E. Canfield, The early history of atmospheric oxygen: Homage to Robert A. Garrels. *Annu. Rev. Earth Planet. Sci.* **33**, 1–36 (2005).
50. D. L. Huston, G. A. Logan, Barite, BIFs and bugs: Evidence for the evolution of the Earth's early hydrosphere. *Earth Planet. Sci. Lett.* **220**, 41–55 (2004).
51. C. T. Reinhard, R. Raiswell, C. Scott, A. D. Anbar, T. W. Lyons, A late Archean sulfidic sea stimulated by early oxidative weathering of the continents. *Science* **326**, 713–716 (2009).
52. H. E. Frimmel, Archaean atmospheric evolution: Evidence from the Witwatersrand gold fields, South Africa. *Earth Sci. Rev.* **70**, 1–46 (2005).
53. J. D. Morris, J. G. Ryan, "2.11–Subduction zone processes and implications for changing composition of the upper and lower mantle" in *Treatise on Geochemistry*, H. D. Holland, K. K. Turekian, Eds. (Pergamon, Oxford, U.K., 2003), pp. 451–470.
54. C. Herzberg, K. Condie, J. Korenaga, Thermal history of the Earth and its petrological expression. *Earth Planet. Sci. Lett.* **292**, 79–88 (2010).
55. J. Korenaga, Initiation and evolution of plate tectonics on Earth: Theories and observations. *Annu. Rev. Earth Planet. Sci.* **41**, 117–151 (2013).
56. C. B. Keller, B. Schoene, Statistical geochemistry reveals disruption in secular lithospheric evolution about 2.5 Gyr ago. *Nature* **485**, 490–493 (2012).
57. B. Keller, B. Schoene, Plate tectonics and continental basaltic geochemistry throughout Earth history. *Earth Planet. Sci. Lett.* **481**, 290–304 (2018).
58. X.-M. Yang, Using the Rittmann Serial Index to define the alkalinity of igneous rocks. *Neues Jahrb. Miner. Abh.* **184**, 95–103 (2007).
59. A. P. Gumsley *et al*., Timing and tempo of the Great Oxidation Event. *Proc. Natl. Acad. Sci. U.S.A.* **114**, 1811–1816 (2017).
60. D. Lahondère, D. Thiéblemont, M. Tegyey, C. Guerrot, B. Diabate, First evidence of early Birimian (2.21 Ga) volcanic activity in Upper Guinea: The volcanics and associated rocks of the Niani suite. *J. Afr. Earth Sci.* **35**, 417–431 (2002).
61. E. L. Klein *et al*., Geochronology, Nd isotopes and reconnaissance geochemistry of volcanic and metavolcanic rocks of the São Luís Craton, northern Brazil: Implications for tectonic setting and crustal evolution. *J. South Am. Earth Sci.* **27**, 129–145 (2009).
62. X. Liu *et al*., Geochronology, redox-state and origin of the ore-hosting porphyry in the Tongkuangyu Cu deposit, North China Craton: Implications for metallogenesis and tectonic evolution. *Precambrian Res.* **276**, 211–232 (2016).
63. E. Meng *et al*., Paleoproterozoic metavolcanic rocks in the Ji'an Group and constraints on the formation and evolution of the northern segment of the Jiao-Liao-Ji Belt, China. *Precambrian Res.* **294**, 133–150 (2017).
64. A. Bekker, H. D. Holland, Oxygen overshoot and recovery during the early Paleoproterozoic. *Earth Planet. Sci. Lett.* **317**, 295–304 (2012).
65. R. Frei, C. Gaucher, S. W. Poulton, D. E. Canfield, Fluctuations in Precambrian atmospheric oxygenation recorded by chromium isotopes. *Nature* **461**, 250–253 (2009).
66. S. Zhang *et al*., Sufficient oxygen for animal respiration 1,400 million years ago. *Proc. Natl. Acad. Sci. U.S.A.* **113**, 1731–1736 (2016).
67. P. W. Crockford *et al*., Triple oxygen isotope evidence for limited mid-Proterozoic primary productivity. *Nature* **559**, 613–616 (2018).
68. C. T. A. Lee *et al*., Two-step rise of atmospheric oxygen linked to the growth of continents. *Nat. Geosci.* **9**, 417–424 (2016).
69. C. J. Hawkesworth, P. A. Cawood, B. Dhuime, T. I. S. Kemp, Earth's continental lithosphere through time. *Annu. Rev. Earth Planet. Sci.* **45**, 169–198 (2017).
70. S. B. Shirey, S. H. Richardson, Start of the Wilson cycle at 3 Ga shown by diamonds from subcontinental mantle. *Science* **333**, 434–436 (2011).
71. M. Tang, K. Chen, R. L. Rudnick, Archean upper crust transition from mafic to felsic marks the onset of plate tectonics. *Science* **351**, 372–375 (2016).
72. H. Liu, Dataset and computer code for the calculation of secular Th/U variations of arc igneous rocks. Oxygen. https://github.com/CodrIocas/Oxygen.git. Deposited 15 August 2019.
73. C. Amante, B. W. Eakins, ETOPO1 arc-minute global relief model: Procedures, data sources and analysis. NOAA Technical Memorandum (National Geophysical Data Center, National Oceanic and Atmospheric Administration, Boulder, CO, 2009), pp. 1–19.
74. C. T. Reinhard, N. J. Planavsky, T. W. Lyons, Long-term sedimentary recycling of rare sulphur isotope anomalies. *Nature* **497**, 100–103 (2013).

Downloaded at Australian Natl Univ on November 5, 2019